IARJSET

ISSN (Online) 2393-8021
ISSN (Print) 2394-1588

International Advanced Research Journal in Science, Engineering and Technology
Vol. 3, Issue 5, May 2016

Molecular Structure, Vibrational Spectra [FT-IR and FT-Raman], Electronic Spectra [UV-Visible] and NMR Analysis on Hydroquinone Using HF and DFT Calculations

R. Durga[1], S.Anand[1], K. Rajkumar[1], S. Ramalingam[1], R.S. Sundararajan[2]

Department of Physics, A.V.C. College, Mayiladuthurai, Tamilnadu, India[1]

Department of Physics, Government Arts College, Kumbakonam, Tamilnadu, India[2]

Abstract: The FT-IR spectrum of Hydroquinone was recorded in the region 4000–100 cm^{-1}. The FT-Raman spectrum of Hydroquinone was also recorded in the region 4000–100 cm^{-1}. Quantum chemical calculations of energies, geometrical structure and vibrational wave numbers of Hydroquinone were carried out by HF and DFT methods with 6-311++G(d,p) basis sets and the corresponding results were tabulated. The difference between the observed and scaled wave number values of most of the fundamentals is very small. Moreover, ^{13}C NMR and ^{1}H NMR were calculated by using the gauge independent atomic orbital method with B3LYP methods and the 6-311++G(d,p) basis set and their spectra were simulated and the chemical shifts linked to TMS were compared. A study on the electronic and optical properties; absorption wavelengths, excitation energy, dipole moment and frontier molecular orbital energies were carried out. The kubo energy gap of the present compound was calculated related to HOMO and LUMO energies which confirm the occurring of charge transformation. Besides Frontier Molecular Orbital's (FMO), Molecular Electrostatic Potential was performed. The NLO properties related to Polarizability and hyperpolarizability based on the finite-field approach were also discussed. A detailed interpretation of the infrared and Raman spectra of Hydroquinone is also reported based on total energy distribution. The calculated HOMO and LUMO energies shows that charge transfer occur within the molecule. The theoretical FT-IR and FT-Raman spectra for the title compound have also been constructed. The thermodynamic properties (heat capacity, entropy and enthalpy) of the title compound at different temperatures were calculated in gas phase.

Key words: Hydroquinone; HOMO-LUMO; optical properties; GIAO; NLO; Chemical shifts.

1. INTRODUCTION

Hydroquinone is an organic compound consisting of a molecular geometry changes due to enhanced interaction between the aromatic ring and hydroxyl group. Molecular organic compounds with one or more aromatic systems in conjugated positions leading to charge transfer systems, have been intensely studied for past two decades. Now-a-days organic crystals are highly recognized as the materials of the future because their molecular nature combined with versatility of synthetic chemistry can be used to alter their structure in order to maximize the non-linear properties [1–3]. The substituted benzene derivatives with high optical non-linearity are very promising materials for future optoelectronic and non-linear optical applications. Particularly, the new non-linear optical crystal of oxygen and hydro substituted benzene has been grown by low temperature solution growth technique. The optical transparency of this crystal is quite good and hence it can be a potential material for frequency doubling of non-linear optics [4]. They have been extensively used for the extraction and analytical determinations of structural analogues of Hydroquinone. They have also been found to exhibit interesting biological properties. Its derivatives attract attention not only because of their role in structure, but also because of exhibited pharmaceutical activities such as intermediate of photo chemicals, rubber, dyes and invoke much interest among the spectroscopists owing to their noval bioactivities such as treatment of analgesic (or) prophylaxis, hemostatic, antiprurite, antitussive, antiasthmatic and also used as a solvent in shoes and metal polishes and in screen printing. When substituted benzene molecules undergo electrophilic substitution reactions, substituents on a benzene ring can influence the reactivity. The inclusion of substituent's in benzene leads to the variation of charge distribution in the molecule, and consequently affects the structural, electronic and vibrational parameters. Therefore, the present investigation has undertaken to study the vibrational spectra, geometrical frame work review, inter and intra molecular interaction between HOMO and LUMO energy levels and first order hyperpolarizability of non linear optical (NLO) activity and other thermodynamic parameters of Hydroquinone molecule. These parameters were investigated by using HF and DFT calculations with 6-311+G(d,p) basis sets. Specific scale factors were also used and employed in the predicted frequencies. It should be emphasized that in our calculations we have included polarization functions on hydrogen atoms, which are known to be very important for

IARJSET
ISSN (Online) 2393-8021
ISSN (Print) 2394-1588
International Advanced Research Journal in Science, Engineering and Technology
Vol. 3, Issue 5, May 2016

reproducing the out-of-plane vibrations involving hydrogen atoms. It is anticipated that both HF and DFT level of theories are reliable for predicting the vibrational spectra of Hydroquinone. The DFT calculations are reported [5] to provide accurate vibrational frequencies of organic compounds if the calculated frequencies are scaled to compensate for the approximate treatment of electron correlation for basis set deficiencies and for the anharmonicity effect [6–10]. Hydroquinone has a variety of uses principally associated with its action as a reducing agent that is soluble in water. It is a major component in most black and white photographic developers for film and paper where, with the compound Metal, it reduces silver halides to elemental silver. There are various other uses associated with its reducing power. As a polymerization inhibitor, hydroquinone prevents polymerization of acrylic acid, methyl methacrylate, cyanoacrylate, and other monomers that are susceptible to radical-initiated polymerization. This application exploits the antioxidant properties of hydroquinone.

2. EXPERIMENTAL METHODS

The title compound is purchased from Sigma–Aldrich Chemicals, USA, which is of spectroscopic grade and hence used for recording the spectra as such without any further purification. The FT-IR spectrum of the compound is recorded in Bruker IFS 66V spectrometer in the range of 4000–100 cm^{-1}. The spectral resolution is ±2 cm^{-1}. The FT-Raman spectrum of AMS is also recorded in the same instrument with FRA 106 Raman module equipped with Nd:YAG laser source operating at 1.064 µm line widths with 200 mW power. The spectra are recorded in the range of 4000–100 cm^{-1} with scanning speed of 30 cm^{-1} min^{-1} of spectral width 2 cm^{-1}. The frequencies of all sharp bands are accurate to ±1 cm^{-1}. The absorption spectrum of Hydroquinone is recorded using Varion Cary 5E UV-Vis-NIR spectrophotometer in the range 200 – 700 nm with high resolution.

3. COMPUTATIONAL METHODS

The molecular structure optimization of the title compound and the corresponding vibrational harmonic frequencies were performed using DFT with Becke-3-Lee-Yang-Parr (B3LYP) [11,12] combined with 6-311++G(d,p) basis sets using GAUSSIAN O9W [13] program package. In DFT methods; Becke's three parameter hybrids function combined with the Lee-Yang-Parr correlation function (B3LYP) [14-15], Becke's three parameter exact exchange-function (B3) [16] combined with gradient-corrected correlational functional of Lee, Yang and Parr (LYP) [17-18] and Perdew and Wang (PW91) [18-19] predict the best results for molecular geometry and vibrational frequencies for moderately larger molecules. The calculated frequencies are scaled down to yield the coherent with the observed frequencies. The scaling factors are 0.89, 0.92 and 0.97 for HF/6-311++G(d,p) method. For DFT/6-311++G(d,p) basis set, the scaling factors are 0.96, 0.97, 0.98 and 0.99. The observed (FT-IR and FT-Raman) and calculated vibrational frequencies and vibrational assignments are submitted in Table 2. Experimental and simulated spectra of IR and Raman are presented in the Figures 2 and 3, respectively.

The electronic properties, such as HOMO-LUMO energies, absorption wavelengths and oscillator strengths are calculated using B3LYP method of the time-dependent DFT (TD-DFT) [20-21], based on the optimized structure in solvent (DMSO, chloroform and CCl_4) and gas phase. The thermodynamic properties of the title compound at different temperatures have been calculated in gas phase using B3LYP/6-311++G (d, p) method. Moreover, the dipole moment, nonlinear optical (NLO) properties, linear polarizabilities and first order hyperpolarizabilities and chemical hardness have also been studied.

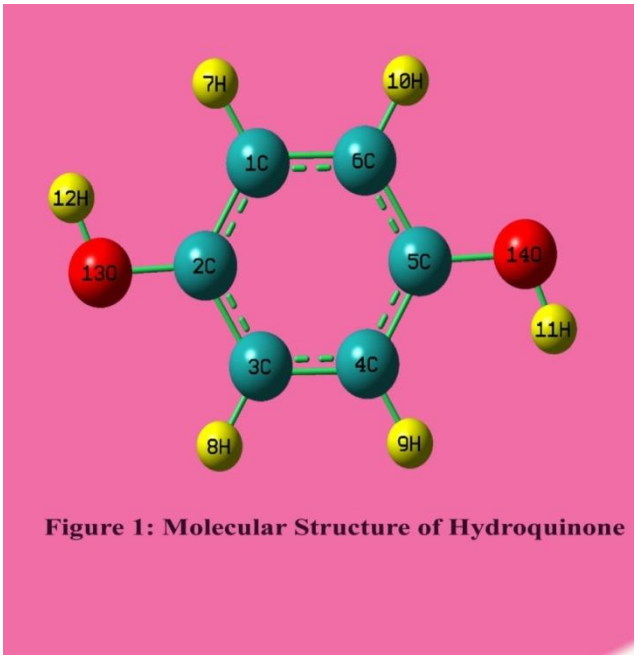

Figure 1: Molecular Structure of Hydroquinone

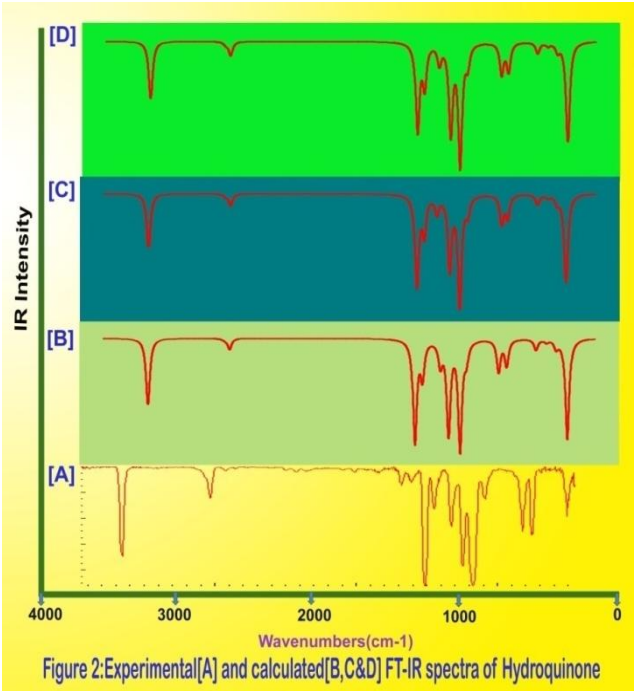

Figure 2:Experimental[A] and calculated[B,C&D] FT-IR spectra of Hydroquinone

IARJSET
ISSN (Online) 2393-8021
ISSN (Print) 2394-1588
International Advanced Research Journal in Science, Engineering and Technology
Vol. 3, Issue 5, May 2016

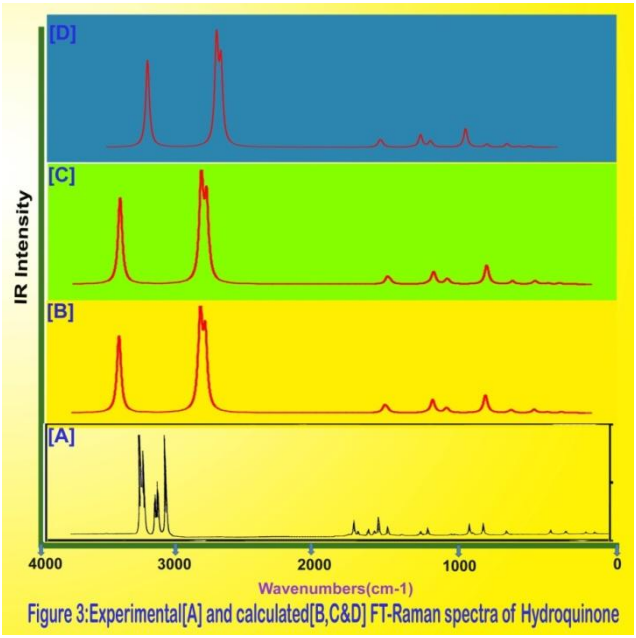

Figure 3:Experimental[A] and calculated[B,C&D] FT-Raman spectra of Hydroquinone

The ^{1}H and ^{13}C NMR isotropic shielding are calculated with the GIAO method [22] using the optimized parameters obtained from B3LYP/6-311++G(d,p) method. ^{13}C isotropic magnetic shielding (IMS) of any X carbon atoms is made according to value ^{13}C IMS of TMS, $CS_X=IMS_{TMS}$. The ^{1}H and ^{13}C isotropic chemical shifts of TMS at B3LYP methods with 6-311++G(d,p) level using the IEFPCM method in DMSO, chloroform and CCl_4. The absolute chemical shift is found between isotropic peaks and the peaks of TMS [23].

4. RESULTS AND DISCUSSION

4.1. Molecular geometry Analysis

The molecular structure of Hydroquinone belongs to C_s point group symmetry. The optimized molecular structure of the molecule is obtained from Gaussian 09 and Gauss view program and is shown in Figure 1. The molecule contains two OH groups connected with benzene ring. The comparative optimized structural parameters such as bond lengths, bond angles and dihedral angles are listed in Table 1. However, the DFT/6-311+G(d,p) level of theory, in general slightly over estimates bond lengths but it yields bond angles in excellent agreement with the HF method. The calculated geometric parameters can be used as foundation to calculate the other parameters for the compound. The structure optimization and zero point vibrational energy of the compound in HF/DFT (B3LYP, B3PW91, CAM-B3LYP and LSDA)/6-311++G(d,p) basic set are 72.44, 67.58, 67.88, 68.43 and 66.23 Kcal/Mol respectively. The calculated energy of HF is greater than DFT method because the assumption of ground state energy in HF is greater than the true energy.

The ring carbon atoms in substituted benzenes exert a larger attraction on the valence electron cloud of the hydrogen atom resulting in an increase in the C–H force constants and a decrease in the corresponding bond length. It is evident from the C–C bond lengths ranging from 1.3822 to 1.3846 Å by HF method and from 1.3924 to 1.3954 Å by DFT (B3LYP) method in the benzene ring of Hydroquinone, whereas the C–H bond lengths in hydroquinone vary from 1.0744 to 1.9079 Å and from 1.0861 to 1.9251 Å by HF and DFT (B3LYP) methods, respectively. The benzene ring appears to be a little distorted because of the OH group substitution as seen from the bond angles C3–C4–C5, which are calculated as 120.496° and 120.415°, respectively, by HF and B3LYP methods and are larger than typical hexagonal angle of 120°.

4.2. Vibrational Analysis

The Hydroquinone molecule consists of 14 atoms, which undergoes 36 normal modes of vibrations. On the assumption of C_s group of symmetry, the number of vibration modes of the 36 fundamental vibrations of the molecule can be distributed as

$$\Gamma Vib = 23\,A' + 13\,A''$$

The A' and A'' species represent the in-plane and out-of plane vibrations, respectively. The harmonic vibrational frequencies (unscaled and scaled) calculated at DFT (B3LYP, CAM-B3LYP, LSDA and B3PW91) and HF levels using the triple split valence basis set along with the diffuse and polarization functions, 6-311++G(d,p) and the observed FT-IR and FT-Raman frequencies for various modes of vibrations have been presented. In comparison of frequencies calculated at HF and DFT with the experimental values reveal the over estimation of the calculated vibrational modes due to the neglect of a harmonicity in real system. Inclusion of electron correlation in the density functional theory to certain extents makes the frequency values smaller in comparison with the HF frequency data. Reduction in the computed harmonic vibrations, although basis set sensitive is only marginal as observed in the DFT values using 6-311++G(d,p). The experimental and calculated frequencies and their assignments are presented in the Tables 2 and 3 and their experimental and simulated spectra of IR and Raman are presented in the Figures 2 and 3 respectively.

4.2.1. C–H vibrations

The aromatic organic compounds structure; benzene and its derivatives show the presence of asymmetric C-H stretching vibrations in the region 3100-3000 cm^{-1} [24-26] which is the characteristics region for recognition of C-H stretching vibrations. In the title molecule, three bands have been observed at 3090, 3050, 3040 cm^{-1} assigned to C-H stretching vibrations. The entire vibrations are observed at the middle of the expected region. This view clearly shows that these stretchings do not affected by the substitutions of atoms. Normally, the strongest absorptions for aromatic compounds occur in the region 1300-1000 cm^{-1} and 1000–750 cm^{-1} due to the C–H in-plane and out-of-plane bending vibrations respectively [27-31]. In the present case, the in-plane bending vibrations are found at 1278, 1245, 1207, 1170, 1095, 1040 and 1020 cm^{-1} in FT-IR and FT-Raman. The entire in-plane bending vibrations are found at the lower end of the expected region. The out-

IARJSET
ISSN (Online) 2393-8021
ISSN (Print) 2394-1588
International Advanced Research Journal in Science, Engineering and Technology
Vol. 3, Issue 5, May 2016

Table 1: Optimized geometrical parameters for Hydroquinone computed at HF, DFT (B3LYP& B3PW91), CAM – B3LYP and LSDA with 6-311++G(d,p) basis sets

Geometrical Parameters	Methods				
	HF	B3LYP	B3PW91	CAM – B3LYP	LSDA
	6-311++G (d-p)	6-311++G (d-p)	6-311++G (d- p)	6-311++G (d-p)	6-311++G (d-p)
		Bond length(Å)			
(C1 - C2)	1.3846	1.3954	1.3936	1.3891	1.3892
(C1 - C6)	1.3845	1.3924	1.3898	1.3868	1.3838
(C1 - H7)	1.0772	1.0861	1.0871	1.0853	1.0962
(C2 - C3)	1.3822	1.393	1.3912	1.3866	1.3869
(C2 - H12)	1.9079	1.9251	1.9143	1.922	1.9106
(C3 - C4)	1.3845	1.3924	1.3898	1.3868	1.3838
(C3 - H8)	1.0744	1.0831	1.0841	1.0825	1.0928
(C4 - C5)	1.3846	1.3954	1.3936	1.389	1.3892
(C4 - H9)	1.0772	1.0861	1.0871	1.0854	1.0962
(C5 - C6)	1.3823	1.393	1.3913	1.3866	1.3869
(C5 - H11)	1.9078	1.925	1.9145	1.9222	1.9111
(C6 - H10)	1.0744	1.0831	1.0841	1.0825	1.0928
(H11 - O14)	0.9402	0.9624	0.9607	0.9606	0.9723
(H12 - O13)	0.9402	0.9623	0.9607	0.9606	0.9722
		Bond angle(˚)			
(C2 - C1 - C6)	120.4961	120.4151	120.5056	120.3748	120.6003
(C2 - C1 - H7)	120.1183	120.0808	120.0674	120.0577	119.7844
(C6 - C1 - H7)	119.3856	119.5041	119.4269	119.5675	119.6153
(C1 - C2 - C3)	119.3399	119.5462	119.3936	119.5873	119.3393
(C1 - C2 - H12)	95.427	94.8358	94.6737	94.8045	94.1303
(C3 - C2 - H12)	145.2329	145.618	145.9326	145.6082	146.5304
(C2 - C3 - C4)	120.1641	120.039	120.0996	120.0358	20.0607
(C2 - C3 - H8)	119.2449	119.2062	119.1787	119.0987	118.8435
(C4 - C3 - H8)	120.591	120.7548	120.7217	120.8655	121.0958
(C3 - C4 - C5)	120.4961	120.4155	120.5101	120.3777	20.5995
(C3 - C4 - H9)	119.384	119.5028	119.4234	119.5665	119.6155
(C5 - C4 - H9)	120.1199	120.0817	120.0665	120.0557	119.785
(C4 - C5 - C6)	119.3401	119.545	119.3881	119.5856	119.3397
(C4 - C5 - H11)	95.4168	94.8212	94.664	94.8115	94.1508
(C6 - C5 - H11)	145.2428	145.6338	145.9479	145.6028	146.5094
(C1 - C6 - C5)	120.1637	120.0391	120.103	120.0388	120.0604
(C1 - C6 - H10)	120.5923	120.7552	120.7201	120.864	21.0966
(C5 - C6 - H10)	119.244	119.2057	119.1769	119.0972	118.843
(C5 - H11 - O14 - C4 -C1)	109.7319	110.7476	111.1894	110.3473	111.1571
(C2 - H12 - O13 - C1 -C1)	109.7161	110.7274	111.1886	110.363	111.2123
(C5 - H11 - O14 - C4 - C2)	359.7736	359.9708	359.9391	0.1397	0.0569
(C2 - H12 - O13 - C1 - C2)	359.8689	359.9287	0.0683	359.9403	0.0448
		Dihedral angles(˚)			
(C6 - C1 - C2 - C3)	0.013	-0.0006	-0.0091	0.0096	-0.0045
(C6 - C1 - C2 - H12)	-179.8958	-179.9669	179.9448	-179.9584	179.9699
(H7 - C1 - C2 - C3)	180.0029	179.9979	179.9922	-179.9831	179.9983
(H7 - C1 - C2 - H12)	0.0941	0.0316	-0.054	0.0489	-0.0273
(C2 - C1 - C6 - C5)	-0.0206	-0.0071	0.0074	-0.0037	0.0062
(C2 - C1 - C6 - H10)	179.9859	179.9961	-179.9976	-179.9965	-179.9963
(H7 - C1 - C6 - C5)	179.9894	179.9945	-179.9939	179.989	-179.9966
(H7 - C1 - C6 - H10)	-0.0041	-0.0023	0.0012	-0.0038	0.0009
(C1 - C2 - C3 - C4)	0.0034	0.0089	0.0068	-0.0151	-0.0022
(C1 - C2 - C3 - H8)	-180.0033	-179.9919	180.0033	179.9972	-179.999
(H12 - C2 - C3 - C4)	179.8442	179.9494	-179.9111	179.9283	-179.9558
(H12 - C2 - C3 - H8)	-0.1625	-0.0514	0.0854	-0.0594	0.0474
(C2 - C3 - C4 - C5)	-0.0124	-0.0097	-0.003	0.0149	0.0072
(C2 - C3 - C4 - H9)	179.9867	179.996	179.9981	-179.9828	180.0054
(H8 - C3 - C4 - C5)	179.9944	179.9912	180.0006	-179.9976	180.0039

DOI 10.17148/IARJSET.2016.3544

IARJSET
ISSN (Online) 2393-8021
ISSN (Print) 2394-1588
International Advanced Research Journal in Science, Engineering and Technology
Vol. 3, Issue 5, May 2016

(H8 - C3 - C4 - H9)	-0.0064	-0.0032	0.0017	0.0047	0.0021
(C3 - C4 - C5 - C6)	0.0049	0.002	0.0012	-0.0089	-0.0054
(C3 - C4 - C5 - H11)	-179.839	180.0391	-179.9731	179.9008	179.9624
(H9 - C4 - C5 - C6)	-179.9942	179.9963	-179.9999	179.9887	179.9963
(H9 - C4 - C5 - H11)	0.1618	0.0334	0.0258	-0.1015	-0.0358
(C4 - C5 - C6 - C1)	0.0115	0.0064	-0.0034	0.0033	-0.0013
(C4 - C5 - C6 - H10)	-179.9949	-179.9968	180.0015	179.9962	180.0012
(H11 - C5 - C6 - C1)	179.739	-180.0591	179.9509	-179.8375	-179.9431
(H11 - C5 - C6 - H10)	-0.2674	-0.0623	-0.0442	0.1555	0.0594

Table 2: Observed and calculated vibrational frequencies of Hydroquinone computed at HF, DFT (B3LYP & B3PW91), CAM – B3LYP and LSDA with 6-311++G(d,p) basis sets

S. No	Symmetry Species C_S	Observed Frequency(cm^{-1})		Methods					Vibrational Assignments
				HF	B3LYP	B3PW91	CAM–B3LYP	LSDA	
		FTIR	FT-Raman	6-311++G (d, p)	6-311++G (d, p)	6-311++G (d, p)	6-311++G (d, p)	6-311++G (d, p)	
1	A′	3855w	-	3857	3842	3833	3847	3851	**(O – H) υ**
2	A′	3750w	-	3730	3725	3754	3728	3737	**(O – H) υ**
3	A′	3403s	-	3387	3386	3398	3378	3378	**(O – H) υ**
4	A′	-	3180w	3352	3194	3204	3217	3126	**(O – H) υ**
5	A′	-	3090w	3311	3154	3164	3178	3083	**(C – H) υ**
6	A′	3040s	3050w	3044	3025	3035	3017	3019	**(C – H) υ**
7	A′	2011w	-	1997	1996	2001	1994	1995	**(C = C) υ**
8	A′	1856w	-	1845	1840	1840	1851	1846	**(C = C) υ**
9	A′	1636s	1600s	1625	1635	1629	1631	1631	**(C = C) υ**
10	A′	1559s	1500w	1552	1557	1547	1549	1558	**(C = C) υ**
11	A′	1517s	-	1516	1507	1516	1515	1512	**(C – C) υ**
12	A′	1471s	-	1469	1465	1461	1470	1465	**(C – C) υ**
13	A′	1353m	-	1370	1345	1342	1350	1351	**(O – H) δ**
14	A′	-	1340vs	1366	1258	1269	1278	1250	**(O – H) δ**
15	A′	1278s	-	1296	1193	1194	1201	1142	**(C – H) δ**
16	A′	1245s	-	1270	1182	1182	1189	1140	**(C – H) δ**
17	A″	1207s	1210w	1201	1178	1179	1178	1128	**(C – H) δ**
18	A″	-	1170w	1157	1113	1113	1123	1072	**(C – H) δ**
19	A″	1095m	-	1095	1093	1092	1086	1093	**(C – H) δ**
20	A″	-	1040w	1062	932	930	962	881	**(C – H) δ**
21	A″	-	1020w	1016	896	889	924	865	**(C – H) δ**
22	A″	890w	-	928	860	867	878	847	**(O – H) γ**
23	A′	828s	-	919	821	819	844	785	**(O – H) γ**
24	A′	790s	-	903	797	796	818	763	**(O – H) γ**
25	A′	760s	790w	816	761	767	774	756	**(O – H) γ**
26	A′	692m	-	748	663	658	759	641	**(C – H) γ**
27	A′	660m	-	706	658	655	665	639	**(C – H) γ**
28	A″	611s	-	609	606	511	608	489	**(C–C–C) δ**
29	A″	517m	-	517	513	470	515	463	**(C–C–C) δ**
30	A″	-	450w	483	447	445	452	430	**(C–C–C) δ**
31	A′	407w	-	464	421	419	430	409	**(C–C–C) γ**
32	A′	390w	-	403	360	362	370	352	**(C–C–C) γ**
33	A″	-	310w	367	340	341	345	333	**(C–C–C) γ**
34	A″	-	220w	196	257	269	253	298	**(C – H) γ**
35	A″	-	185w	194	251	264	249	292	**(C – H) γ**
36	A″	-	150w	169	153	153	156	148	**(C – H) γ**

s – Strong; m- Medium; w – Weak; vs- Very Strong; υ – stretching;
δ - In plane bending; γ – out plane bending

DOI 10.17148/IARJSET.2016.3544

IARJSET
ISSN (Online) 2393-8021
ISSN (Print) 2394-1588
International Advanced Research Journal in Science, Engineering and Technology
Vol. 3, Issue 5, May 2016

Table 3: Calculated unscaled frequencies of Hydroquinone computed at HF, DFT (B3LYP& B3PW91), CAM – B3LYP and LSDA with 6-311++G(d,p) basis sets

S. No	Observed frequency	Calculated frequency				
		HF 6-311++G (d, p)	B3LYP 6-311++G (d, p)	B3PW91 6-311++G (d, p)	CAM–B3LYP 6-311++G (d, p)	LSDA 6-311++G (d, p)
1	3855	4193	3842	3872	3886	3739
2	3750	4192	3841	3871	3884	3737
3	3403	3354	3195	3206	3218	3128
4	3180	3352	3194	3204	3217	3126
5	3090	3311	3154	3164	3178	3083
6	3040	3309	3152	3162	3176	3081
7	2011	1816	1664	1682	1705	1663
8	1856	1792	1643	1658	1683	1634
9	1636	1676	1543	1552	1569	1525
10	1559	1601	1483	1488	1504	1457
11	1517	1472	1358	1379	1365	1414
12	1471	1386	1357	1353	1349	1320
13	1353	1370	1281	1303	1311	1287
14	1340	1366	1258	1269	1278	1250
15	1278	1296	1193	1194	1201	1142
16	1245	1270	1182	1182	1189	1140
17	1207	1201	1178	1179	1178	1128
18	1170	1157	1113	1113	1123	1072
19	1095	1097	1022	1021	1035	994
20	1040	1062	932	930	962	881
21	1020	1016	896	889	924	865
22	890	928	860	867	878	847
23	828	919	821	819	844	785
24	790	903	797	796	818	763
25	760	816	761	767	774	756
26	660	748	663	658	684	641
27	692	706	658	655	665	639
28	611	570	510	511	520	489
29	517	504	471	470	477	463
30	450	483	447	445	452	430
31	407	464	421	419	430	409
32	390	403	360	362	370	352
33	310	367	340	341	345	333
34	220	196	257	269	253	298
35	185	194	251	264	249	292
36	150	169	153	153	156	148

of-plane bending vibrations are observed at 692 and 660 cm^{-1}. Most of the bending vibrations are found in IR and except one, all the bending bands are within the expected region. This view indicates that the substitutions in the ring have influenced slightly the out-of-plane bending vibrations. The C-H out-of-plane bending vibrations are appeared at 220, 185 and 150 cm^{-1} respectively. These vibrations are affected much by other vibrations which make disagreement with literature values.

4.2.2. C–C vibrations

The ring stretching vibrations are very much important in the spectrum of benzene and its derivatives are highly characteristic of the aromatic ring itself. The ring C=C and C–C stretching vibrations, known as semicircle stretching usually occur in the region 1625-1400 cm^{-1}. Particularly, the bands between the regions 1590-1650 cm^{-1} [32] and 1590-1430 cm^{-1} [33-34] in benzene derivatives are usually assigned to C=C and the C–C stretching vibrations respectively. In the present case, the C=C stretching vibrations are observed with strong intensity at 1636 and 1559 cm^{-1} and weak intensity at 2011 and 1856 cm^{-1}. The corresponding C–C stretching vibrations are found with strong intensity at 1517 and 1471 cm^{-1}. In the present compound, the C-C-C in-plane and out-of-plane bending vibrations are appeared strong and medium intensity at 611, 517 & 450 cm^{-1} and 407, 390 & 310 cm^{-1} respectively. All the assignments related to in-plane and out-of-plane ring bending vibrations are in coherent with the literature values.

DOI 10.17148/IARJSET.2016.3544

IARJSET
ISSN (Online) 2393-8021
ISSN (Print) 2394-1588
International Advanced Research Journal in Science, Engineering and Technology
Vol. 3, Issue 5, May 2016

4.2.3. O–H Vibrations

The O-H vibrations are generally measured between 3600-3200 cm^{-1} [35]. The O-H stretching vibrations are observed at strong and weak intensity of Hydroquinone at 3403 and 3180 cm^{-1}. In the candidate molecule, the stretching vibration is observed with strong band at 3403 cm^{-1} which is in conformity with the literature. Also, the two weak bands are observed in 3855 and 3750 cm^{-1}. The in-plane bending vibration occurs between the ranges 1350-1200 cm^{-1}. Here too, the in-plane vibrations are found at 1353 and 1340 cm^{-1} in the expected range. In the same way, the out-of-plane vibrations are generally observed at 900 -700 cm^{-1} [36]. In the present molecule, the out-of-plane vibrations are observed at 890, 828, 790 and 760 cm^{-1}, which is also found in the expected range. Thus the O-H vibrations on the whole are not affected in any way by the vibrations of phenyl ring or ethyl or methyl group of the molecule.

4.3. NMR analysis

NMR spectroscopy technique is throwing new light on organic structure elucidation of much difficult complex molecules. The combined use of experimental and computational tools offers a powerful gadget to interpret and predict the structure of bulky molecules. In this way, the optimized structure of Hydroquinone is used to calculate the NMR spectra at B3LYP method with 6-311++G(d,p) level using the GIAO method and the chemical shifts of the compound are reported in ppm relative to TMS for ^{1}H and ^{13}C NMR spectra which are presented in Table 4. The corresponding spectra are shown in Figure 4.

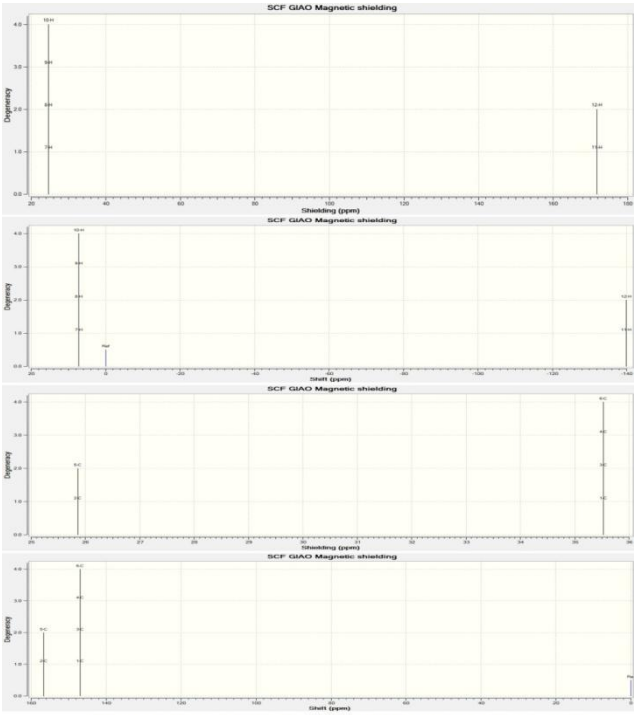

Figure 4: Simulated 13C & 1H NMR spectra of Hydroquinone

Normally, the range of ^{13}C NMR chemical shifts is greater than 100 ppm [37-38] and the accuracy ensure that the reliable interpretation of spectroscopic parameters. In the present work, ^{13}C NMR chemical shifts of entire carbons in the ring are above 100 ppm, as in the expected regions. The present molecule posses hexagonal ring, in which the chemical shift of C1 =C3 =C4 =C6 =111.40 ppm and C2= C5=130.74 ppm. The chemical shifts of C2 and C5 are more than the rest of others. This is mainly due to the breaking of paramagnetic shield of proton by the substitutions of OH group. The chemical shift of H7, H8, H9, H10 are equal and its value is 17.39 ppm and that of H11 and H12 are equal to 31.89 ppm. From the result of shift of Hydrogen atom, it is observed that, the chemical shift of H11 and H12 are higher than the rest of other hydrogen atoms in the chain. This is purely due to the extended influence on hydrogen atom by nearby hydroxyl groups. From the entire chemical shift of the molecules, it can be inferred that, the chemical property of the hydroxyl group is directly mingled with organic molecules and this is the main cause for the present molecule having new chemical property.

4.4 Electronic and Optical properties (HOMO-LUMO) Analysis

The probable transitions in electronic-vibrational energy levels of frontier molecular orbitals are used to identify the electro-optical properties of the organic compounds. The overlapping of molecular orbitals in bonding and antibonding is used in making the stabilization of orbital [39]. In molecular interaction, there are two important orbitals that involved in interacting with each other. They are HOMO and LUMO. HOMO is the highest energy occupied molecular orbital that represents the ability to donate an electron. LUMO is the lowest energy unoccupied molecular orbital that represents the ability to accept an electron. These molecular orbitals are also called the frontier molecular orbitals. The interaction between them is much stable and is called filled empty interaction. During the interaction, the electron density is generally occupied in the region between two nuclei. The energy of in-phase interaction is greater than the out-of-phase interaction and forms bonding and antibonding molecular orbital. The 3D view of frontier orbitals in gas is shown in Figure 5. From this observation, it is clear that, the in- and out-of-phase interactions are present in HOMO and LUMO respectively. The HOMO→LUMO transition implies an electron density transferred among carbon and OH separately. The HOMO and LUMO energy are 5.8845 eV and 0.6887 eV in gas phase (Table 5). Energy difference between HOMO and LUMO orbital is called as energy gap (kubo gap) that is an important feature for the stability of structures. The DFT level calculated energy gap is 5.1958 eV, which is considerably high and hence the present compound is chemically stable. This high value of energy gap reflects the electrical activity of the title molecule to be high.

In order to understand electronic transitions of the compound, time-dependent DFT (TD-DFT) calculations on electronic absorption spectrum in vacuum and solvent (DMSO, Chloroform and CCl_4) are performed by B3LYP / 6-311 ++ G (d, p) basis set. The calculated

IARJSET

ISSN (Online) 2393-8021
ISSN (Print) 2394-1588

International Advanced Research Journal in Science, Engineering and Technology
Vol. 3, Issue 5, May 2016

Table 4: Calculated 1H and 13C NMR chemical shifts (ppm) of Hydroquinone

Atom position	B3LYP/6-311+G (d,p) (ppm)	TMS B3LYP/6-311+G (2d,p) GIAO (ppm)	Shift (ppm)	B3LYP/6-311+G (d,p) (ppm)	TMS B3LYP/6-311+G (2d,p) GIAO (ppm)	Shift (ppm)	B3LYP/6-311+G (d,p) (ppm)	TMS B3LYP/6-311+G (2d,p) GIAO (ppm)	Shift (ppm)	B3LYP/6-311+G (d,p) (ppm)	TMS B3LYP/6-311+G (2d,p) GIAO (ppm)	Shift (ppm)
	Gas			DMSO			Chloroform			CCl4		
C1	35.53	146.93	111.40	35.53	146.59	111.06	35.92	146.54	110.62	35.88	146.58	110.70
C2	25.86	156.60	130.74	11.13	171.33	160.00	15.36	167.10	151.74	19.41	163.04	143.63
C3	35.53	146.93	111.40	35.53	146.59	111.06	35.92	146.54	110.62	35.88	146.58	110.70
C4	35.53	146.93	111.40	35.53	146.59	111.06	35.92	146.54	110.62	35.88	146.58	110.70
C5	25.86	156.60	130.74	11.13	171.33	160.00	15.36	167.10	151.74	19.41	163.04	143.63
C6	35.53	146.93	111.40	35.53	146.59	111.06	35.92	146.54	110.62	35.88	146.58	110.70
H7	24.63	7.24	17.39	24.46	7.42	17.04	24.50	7.37	17.13	24.55	7.32	17.23
H8	24.63	7.24	17.39	24.46	7.42	17.04	24.50	7.37	17.13	24.55	7.32	17.23
H9	24.63	7.24	17.39	24.46	7.42	17.04	24.50	7.37	17.13	24.55	7.32	17.23
H10	24.63	7.24	17.39	24.46	7.42	17.04	24.50	7.37	17.13	24.55	7.32	17.23
H11	171.75	139.86	31.89	141.52	109.64	31.88	148.50	116.61	31.89	156.29	124.41	31.88
H12	171.75	139.86	31.89	141.52	109.64	31.88	148.50	116.61	31.89	156.29	124.41	31.88

Table 5: Frontier molecular orbitals with energy levels of Hydroquinone

Energy levels	Energy in eV
H+8	11.8691
H+7	11.5793
H+6	10.8505
H+5	10.7338
H+4	10.3444
H+3	9.5430
H+2	8.7036
H+1	7.2706
H	5.8845
L	0.6887
L-1	0.3527
L-2	0.3456
L-3	0.1211
L-4	0.3401
L-5	0.4229
L-6	0.9968
L-7	1.4925
L-8	1.5124
L-9	1.7921
L-10	2.2191

DOI 10.17148/IARJSET.2016.3544

IARJSET
ISSN (Online) 2393-8021
ISSN (Print) 2394-1588
International Advanced Research Journal in Science, Engineering and Technology
Vol. 3, Issue 5, May 2016

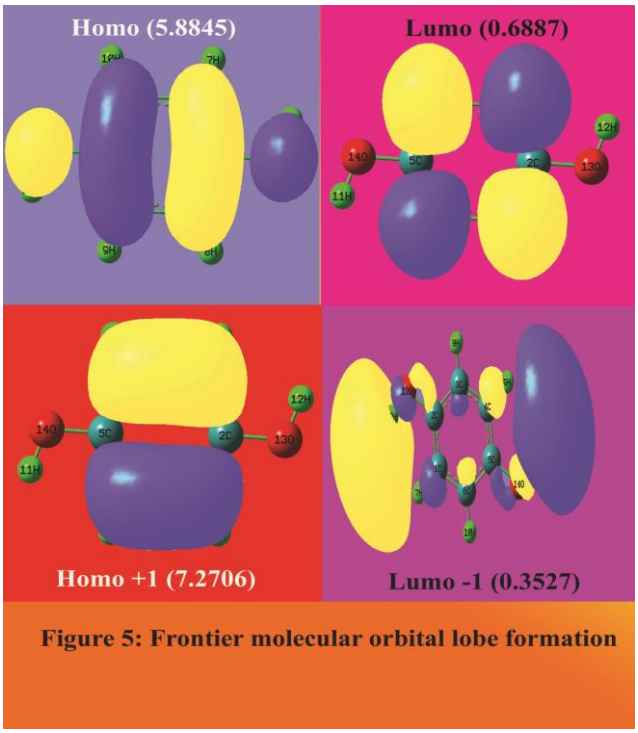

Figure 5: Frontier molecular orbital lobe formation

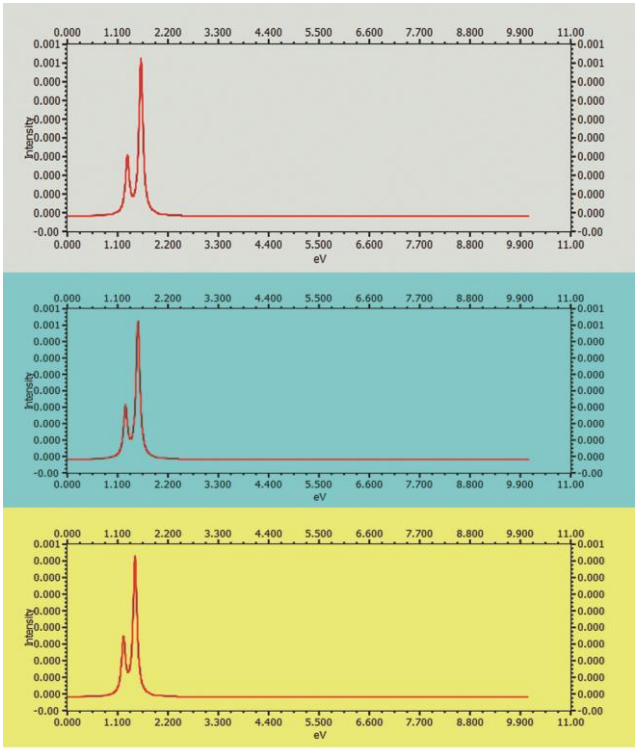

Figure 6: Simulated UV - Visible spectra of Hydroquinone

absorption wavelengths (λ), oscillator strengths (f), excitation energies (E) and dipole moments (μ) are given in Table 6. The strong transitions at 937.20 nm (1.329 eV) with an oscillator strength f=0.0004 in DMSO, at 966.76 nm (1.2825 eV) in chloroform, at 1001.46 nm (1.2380 eV) and at 1068.56 nm (1.1603 eV) in gas phase are assigned to an n→σ* transition. The other wavelength, excitation energies, oscillator strength and calculated counterparts with major contributions are presented in Table 6. The transition is denoted by n→σ* belongs to visible region. The designation of the band is R-band (German, radikalartig) which is attributed to above said transition of chain of aromatic group. They are characterized by low molar absorptivities (ξ_{max}<100) and undergo hypsochromic to bathochromic shift and the solvent effect is inactive in this compound. The simulated UV-Visible spectra in gas and solvent phase are shown in Figure 6.

The chemical hardness and potential, electronegativity and Electrophilicity index are calculated and their values are shown in Table 7. The chemical hardness is a good indicator of the chemical stability. The chemical hardness of the present compound is 2.59 and therefore, the present compound has much chemical stability. Similarly, the electronegativity of the compound is 3.28 and this value is greater than 1.7; due to the presence of hydroxyl group. Electrophilicity index is a factor which is used to measure the energy lowering due to maximal electron flow between donor [HOMO] and acceptor [LUMO]. From the Table 7, it is found that the Electrophilicity index is 3.39×10^{-6} which is high and this value ensures that the strong energy transformation is taking place between HOMO+1 and LUMO-1 instead of HOMO-LUMO since the transition is forbidden between HOMO and LUMO. The dipole moment of a molecule is another important electronic property. Whenever the molecule would have possessing small dipole moment, the intermolecular interactions is very weak. The calculated dipole moment value for the title compound is 0.0042 Debye. It is apparent and moderate due to the presence of weak intermolecular interactions in the molecule.

4.5. Molecular Electrostatic Potential (MEP) Analysis

The molecular electrostatic potential is nothing but the existence of interaction energy between the negative and positive charge distribution of a molecule. The molecular interaction energy was calculated by using the equation

$$V(r_1) = \sum_{j=1}^{M} \frac{Q_i}{\left[r_1 - r_j \right]}$$

If the charge distribution continuous over the compound, the MEP is then given by equation at any instant

$$V(r_1) = \int \frac{\rho(r)}{\left[r_1 - r \right]} dr$$

The MEP is highly informative concerning the protonic and electronic charge distribution of a given molecule. It is mainly used for optical polarization interactions analysis analogous to the crystalline state. It is also used for topographical analysis of the electronic structure and molecular reactivity pattern of the composite materials.The molecular electrostatic potential, V(r), at a given point r (x, y, z) in the environment of a molecule, is defined in terms of the interaction energy between the electrical charge generated from the molecule electrons and nuclei and a positive test charge (a proton) located at r. The molecular electrostatic potential (MEP) is related to the electronic density and is a very useful descriptor for determining sites for electrophilic attack and nucleophilic reactions as well as hydrogen-bonding interactions [40-41]. To predict reactive sites for electrophilic and

IARJSET
ISSN (Online) 2393-8021
ISSN (Print) 2394-1588
International Advanced Research Journal in Science, Engineering and Technology
Vol. 3, Issue 5, May 2016

Table 6: Theoretical electronic absorption spectra of Hydroquinone (absorption wavelength λ (nm), excitation energies E (eV) and oscillator strengths (f)) using TD-DFT/B3LYP/6-311++G(d,p) method

λ (nm)	E (eV)	(*f*)	Major contribution	Assignment	Region	Bands
Gas						
1068.56	1.1603	0.0004	H→L (92%)	n→σ*	visible	R-band (German, radikalartig)
894.24	1.3865	0.0008	H+1→L (86%)	n→σ*	visible	
DMSO						
937.20	1.3229	0.0004	H→L (90%)	n→σ*	visible	R-band (German, radikalartig)
765.84	1.6189	0.0011	H+1→L-1 (83%)	n→σ*	visible	
Chloroform						
966.76	1.2825	0.0004	H→L (86%)	n→σ*	visible	R-band (German, radikalartig)
797.54	1.5546	0.0011	H+1→L-1(77%)	n→σ*	visible	
CCl_4						
1001.46	1.2380	0.0004	H→L (86%)	n→σ*	visible	R-band (German, radikalartig)
831.92	1.4903	0.0010	H+1→L-1(74%)	n→σ*	visible	

H: HOMO; L: LUMO

Table 7: Calculated energies values, chemical hardness, electro negativity, Chemical potential, Electrophilicity index of Hydroquinone

Parameters	TD-DFT/B3LYP/ 6-311G++(d, p)
E_{total} (Hartree)	382.80
E_{HOMO} (eV)	5.8845
E_{LUMO} (eV)	0.6887
$\Delta E_{HOMO\text{-}LUMO\ gap}$ (eV)	5.1958
$E_{HOMO\text{-}1}$ (eV)	1.3861
E_{LUMO+1} (eV)	0.3360
$\Delta E_{HOMO\text{-}1\text{-}LUMO+1\ gap}$ (eV)	1.0501
Chemical hardness (η)	2.5979
Electronegativity (χ)	3.2866
Chemical potential (μ)	2.5979
Chemical softness(S)	0.1924
Electrophilicity index (ω)	3.39×10^{-6}
Dipole moment	0.0042

Table 8: The dipole moments μ (D), the polarizability α (a.u.), the average polarizability αo (esu), the anisotropy of the polarizability Δα (esu), and the first hyperpolarizability β (esu) of Hydroquinone

Parameter	a.u.	Parameter	a.u.
α_{xx}	-44.9200	β_{xxx}	0.0248
α_{xy}	10.4327	β_{xxy}	0.0006
α_{yy}	-39.8237	β_{xyy}	-0.0033
α_{xz}	0.004	β_{yyy}	-0.0015
α_{yz}	0.0005	β_{xxz}	0.0504
α_{zz}	-50.7644	β_{xyz}	0.0122
α_{tot}	100.345	β_{yyz}	0.0024
Δα	156.861	β_{xzz}	0.0007
μ_x	0.0011	β_{yzz}	-0.0005
μ_y	0.0000	β_{zzz}	-0.0001
μ_z	0.0041	β_{tot}	1.5864
μ	0.0043		

DOI 10.17148/IARJSET.2016.3544

IARJSET
ISSN (Online) 2393-8021
ISSN (Print) 2394-1588
International Advanced Research Journal in Science, Engineering and Technology
Vol. 3, Issue 5, May 2016

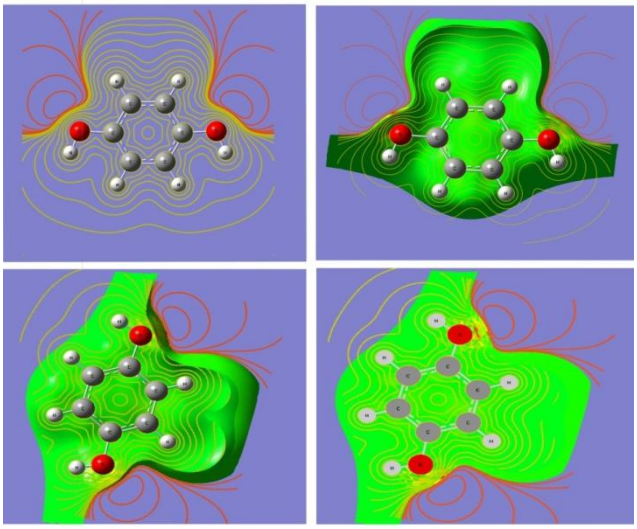

Figure 7: MEP map diagram with isosurface of Hydroquinone

nucleophilic attack for the title molecule, MEP was calculated at the B3LYP/6-311++G(d,p) optimized geometry. The negative (red) regions of MEP were related to electrophilic reactivity and the positive (blue) regions to nucleophilic reactivity as shown in Figure 7. The negative regions are mainly localized on the electronegative atoms. A maximum positive region is localized on the hydrogen group of the molecule indicating a possible site for nucleophilic attack. The addition of electron withdrawing groups produces a large increase in positive potential at the center of the ring. The variance in ESP surfaces shows an increase in the intensity of this localized positive potential in the molecule becomes more electron-deficient. Thus, the ESP surface measurements identify two complementary regions within the compound. Electrophiles (electron-deficient, positively charged species) tend to be attracted to the regions of a molecule in which the ESP attains its most negative values since these are the effects of molecule's electrons are most dominant, whereas nucleophiles (an electron rich, negatively charged species) are especially attracted to the areas where the ESP is the most positive. The contour of electrostatic potential and molecular electrostatic potential are shown in Figure 7.

4.6. Polarizability and First Order Hyperpolarizability Analysis

In order to investigate the relationships among the molecular structures, non-linear optic properties (NLO) and molecular binding properties, the polarizabilities and first order hyperpolarizabilities of the title compound are calculated using DFT-B3LYP method and 6-311+G(d,p) basis set, based on the finite-field approach.

The Polarizability and hyperpolarizability tensors (α_{xx}, α_{xy}, α_{yy}, α_{xz}, α_{yz}, α_{zz} and β_{xxx}, β_{xxy}, β_{xyy}, β_{yyy}, β_{xxz}, β_{xyz}, β_{yyz}, β_{xzz}, β_{yzz}, β_{zzz}) are obtained from the output file of Polarizability and hyperpolarizability calculations. However, α and β values of Gaussian output are in atomic units (a.u.) and have been converted into electronic units (esu) (α; 1 a.u. = 0.1482×10^{-24} esu, β; 1 a.u. = 8.6393×10^{-33} esu). The mean polarizability (α), anisotropy of polarizability (Δα) and the average value of the first order hyperpolarizability $\langle\beta\rangle$ can be calculated using the equations.

$$\alpha_{tot} = \frac{1}{3}\left(\alpha_{xx} + \alpha_{yy} + \alpha_{zz}\right)$$

$$\Delta\alpha = \frac{1}{\sqrt{2}}\left[\left(\alpha_{xx} - \alpha_{yy}\right)^2 + \left(\alpha_{yy} - \alpha_{zz}\right)^2 + \left(\alpha_{zz} - \alpha_{xx}\right)^2 + 6\alpha_{xz}^2 + 6\alpha_{xy}^2 + 6\alpha_{yz}^2\right]^{\frac{1}{2}}$$

$$\langle\beta\rangle = \left[\left(\beta_{xxx} + \beta_{xyy} + \beta_{xzz}\right)^2 + \left(\beta_{yyy} + \beta_{yzz} + \beta_{yxx}\right)^2 + \left(\beta_{zzz} + \beta_{zxx} + \beta_{zyy}\right)^2\right]^{\frac{1}{2}}$$

It is well known that, molecule with low values of dipole moment, molecular Polarizability and first order hyperpolarizability having more active NLO properties. The first order hyperpolarizability (β) and the component of hyperpolarizability β_x, β_y and β_z of Hydroquinone along with related properties (μ_0, α_{total}, and Δα) are reported in Table 8. The calculated value of dipole moment is found to be 0.0043 Debye. The highest value of dipole moment is observed in the component of μ_z which is 0.0041 D. The lowest value of the dipole moment of the molecule is μ_y component (0.0000 D). The calculated average Polarizability and anisotropy of the Polarizability is 100.34 x 10^{-24} esu and 156.86 x 10^{-24} esu, respectively. The high value of Polarizability reflects the rich NLO property of the present compound. The magnitude of the molecular hyperpolarizability β, is one of the important key factors in NLO system. The B3LYP/6-311+G(d,p) calculated first order hyperpolarizability value (β) is 1.5864 x 10^{-30} esu. The hyperpolarizability result explore that, the title compound is able to generate the second order harmonic generation with more amplitude. So, the present compound can be used to prepare the NLO crystals for electronic applications. In addition to that, due to its elevated values of Polarizability and hyperpolarizability, the present compound is able to bind with other molecules with less amount of binding energy.

4.7. Thermodynamic properties

Thermodynamic properties provide the necessary information regarding the chemical reactivity. Moreover,

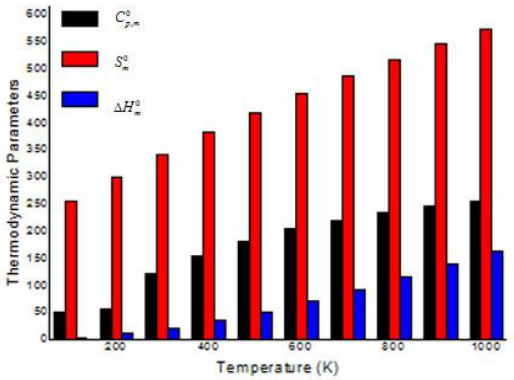

Figure 8: Thermodynamical Parameters at different temperatures

IARJSET
ISSN (Online) 2393-8021
ISSN (Print) 2394-1588
International Advanced Research Journal in Science, Engineering and Technology
Vol. 3, Issue 5, May 2016

Table 9: Thermodynamic parameters at different temperatures at the B3LYP/6-311++G (d, p) level for Hydroquinone

T(K)	$C^0_{p,m}$ (cal mol^{-1} K^{-1})	S^0_m (cal mol^{-1} K^{-1})	ΔH^0_m (kcal mol^{-1})
100.00	49.84	254.16	3.80
200.00	56.54	299.85	10.60
298.15	122.25	341.12	20.87
300.00	122.90	341.88	21.09
400.00	155.51	381.83	35.06
500.00	182.32	419.52	52.00
600.00	203.63	454.72	71.34
700.00	220.61	487.43	92.58
800.00	234.41	517.82	115.35
900.00	245.86	546.11	139.38
1000.00	255.53	572.53	164.47

it is used to discuss the existence and alternation of thermodynamic parameters of the present compound. The values of some thermodynamic parameters such as standard heat capacities ($C^0_{p,m}$), standard entropies (S^0_m) and standard enthalpy changes ($\Delta H^0 m$) of title molecule by B3LYP/6-311++G(d, p) method are listed in Table 9. On the basis of vibrational analysis, these values were obtained from the theoretical harmonic frequencies. From Table 9, it can be observed that these thermodynamic functions are increased with temperature ranging from 100 to 1000 K due to the fact that the molecular vibrational intensities increase with temperature. The correlation graph between heat capacities, entropies, enthalpy changes and temperatures were shown in Figure 8. From this observation, it is clear that, the dissociation of atoms related to the temperature is increased up to 1000 K and the molecule has positive entropy-coefficient. In the case of thermodynamical analysis of the molecule, the enthalpy of a system due to the production of hydrogen ion and organic interactions found be increased with consecutive saturation between successive temperatures. At low temperature, it found that specific heat capacity of present compound falls down rapidly and obeys the Debye T^3 law.

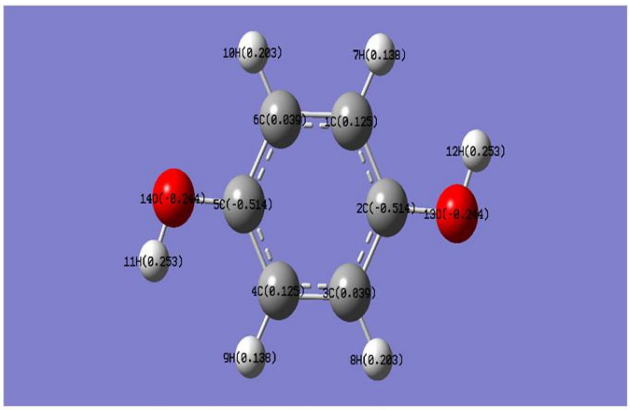

Figure 9: Mulliken Charge of Hydroquinone

Table 10: Mulliken charges for Hydroquinone at HF/6-311G ++ (d,p) basis sets

Atom	Mullikan Charges
C1	0.125
C2	– 0.514
C3	0.039
C4	0.125
C5	– 0.514
C6	0.039
H7	0.138
H8	0.203
H9	0.138
H10	0.203
H11	0.253
H12	0.253
O13	– 0.244
O14	– 0.244

4.8. Mulliken Charge Analysis

The Mulliken charge is used to understand the charge distribution on the chemical bonding because it facilitates positive and negative regions in the molecular space, at which the protons and electrons concentrate. Thus chemically significant regions; bonds can be identified; also gives the narration of the mechanism of electrophilic and nucleophilic substitutions. Normally the charges are distributed evenly over the molecule which leads to be neutral. Whenever the substitutions are added to the molecule, the charge distribution is completely altered with respect to the substitution. The charge distribution on the molecule has an important influence on the vibrational spectra. The calculated Mulliken charge distributions of benzene derivates are presented in Table 10. The results show that the substitution in the aromatic ring by OH group leads to a redistribution of electron density. As can be seen in Table 10, all the hydrogen atoms have a net positive charge. Moreover, the H11 and H12 atoms accommodate higher positive charge than the other hydrogen atoms H7, H8, H9 and H10. The atomic charges of H7 & H9, H8 & H10 and H11 & H12 atoms are also almost identical. The negative charges mainly located on atoms C2 & C5 and these can interact with the positivepart of the receptor. The remaining Carbon atoms have positive charges. The two oxygen atoms in the molecule have negative charge and these can interact with the positive

part of the hydrogen atom. Thus the entire charge levels of the molecule are altered on par with due to the substitution. Simultaneously, the chemical property has also changed for the same. The Mulliken charge analysis diagram is displayed in the Figure 9.

5. CONCLUSION

The FT-IR and FT-Raman spectra were recorded and the detailed vibrational assignments using HF and DFT methods with 6-311++G(d,p) basis sets were made for Hydroquinone. The difference between the corresponding wave numbers (observed and calculated) is very small for most of fundamentals. Therefore, the results presented in this work for Hydroquinone indicate that this level of theory is reliable for the prediction of both Infrared and Raman spectra of the title compound. The simulated ^{13}C NMR and ^{1}H NMR spectra in gas and solvent phase are displayed and the chemical shifts related to TMS are studied. The electrical and optical and bio molecular properties are profoundly investigated using frontier molecular orbital. It is also found that the present compound is optically and electrically active and also posses NLO properties. The electronic excitation in UV-VIS spectra was analyzed. The optimization has been done in order to investigate the energetic behavior and dipole moment of title compound in the gas phase and solvent. The molecular electrostatic potential (MEP) analysis is performed and from which the change of the chemical properties of the compound is also discussed. Furthermore, theoretical calculations have been carried out for the thermodynamic properties (heat capacity, entropy and enthalpy) for the present compound. It was observed that, these thermodynamic functions were increased with temperature due to the fact that the molecular vibrational intensities increased with temperature. From the Mulliken charge analysis, the entire charge levels of the molecule are altered on par with due to the substitution.

REFERENCES

[1] J. Williams (Ed.), Nonlinear Optical Properties of Organic and Polymeric Materials, American Chemical Society Symposium Series, vol. 233, American Chemical Society, Washington, DC, 1983.
[2] D.C. Chemla, J. Zyss (Eds.), Nonlinear Optical Properties of Organic Molecules and Crystals, vol. 1–2, Academic Press, New York, 1987.
[3] N. Vijayan, R. Ramesh Babu, R. Gopalakrishnan, P. Ramasamy, W.T.A. Harrison, J. Cryst. Growth 262 (2004) 490–498.
[4] Y. Goto, A. Hyashi, Y. Kimura, S.M. Nakayama, J. Cryst. Growth 108 (1991) 688–698.
[5] M. Ramalingam, M. Jaccob, J. Swaminathan, P. Venuvanalingam, N. Sundaraganesan, Spectrochim. Acta 71A (2008) 996–1002.
[6] N.C. Handy, C.W. Murray, R.D. Amos, J. Phys. Chem. 97 (1993) 4392–4396.
[7] P.J. Stephens, F.J. Devlin, C.F. Chavalowski, M.J. Frisch, J. Phys. Chem. 98 (1994) 11623–11627.
[8] F.J. Delvin, J.W. Finley, P.J. Stephens, M.J. Frish, J. Phys. Chem. 99 (1995) 16883–16902.
[9] S.Y. Lee, B.H. Boo, Bull. Kor. J. Chem. Soc. 17 (1996) 760–764.
[10] P.B. Nagabalasubramanian, S. Periandy, S. Mohan, Spectrochim. Acta 77 A (2010) 150–159.
[11] A.D. Becke, J. Chem. Phys. 98 (1993) 5648–5652.
[12] C. Lee, W.T. Yang, R.G. Parr, Phys. Rev. B37 (1988) 785–789.
[13] M.J. Frisch, G.W. Trucks, H.B. Schlegal, et al., GAUSSIAN 09. Revision A. 02, Gaussian, Inc., Wallingford, CT, 2009.
[14] D. Hartley and H. Kidd (eds.). The Agrochemicals Handbook. Old Woking, Surrey, United Kingdom: Royal Society of Chemistry / Unwin Brothers Ltd., (1983).
[15] W. Gerhartz, Ullmann's Encyclopedia of Industrial Chemistry. 5th ed: Deerfield Beach, FL: VCH Publishers, 1985 21.
[16] M.K. Marchewka, A. Pietraszko, Spectrochimica Acta Part A 69 (2008) 312–318.
[17] Ivan S. Lim, Gustavo E. Scuseria, Chemical Physics Letters, 460, 2008, 137-140.
[18] Ljupco Pejov, Mirjana Ristova, Bojan Soptrajanov, Spectrochimica Acta Part A 79 (2011) 27–34.
[19] M.J. Frisch et al., Gaussian 09, Revision A.1, Gaussian, Inc., Wallingford CT, 2009.
[20] E. Runge, E. K. U. Gross, Physics Review Letters, 52 (1984) 997-1000.
[21] R. Bauernschmitt, R. Ahlrichs, Chem. Phys. Lett. 256 (1996) 454–464.
[22] Z. Zhengyu, D. Dongmei, Journal of Molecular Structure (Theochem) 505 (2000) 247 252.
[23] Z. Zhengyu, F. Aiping, D. Dongmei, Journal of Quantum Chemistry, 78 (2000) 186-189.
[24] L.J. Bellamy, The Infrared Spectra of Complex Molecules, Chapman and Hall,London, 1975.
[25] George Socrates, Infrared and Raman characteristics group frequencies third edition, wiley, New York (2001).
[26] N. Puviarasan, V. Arjunan, S. Mohan, Turkey Journal of Chemistry, 26 (2002) 323.
[27] G. Varsanyi, Vibrational Spectra of Benzene Derivatives, Academic Press, New York, 1969.
[28] V. Krishnakumar, R.J. Xavier, Indian Journal of Pure and Applied Physics, 41 (2003) 597.
[29] M. Silverstein, G. Clayton Bassler, C. Morrill, Spectrometric Identification of Organic Compounds, Wiley, New York, 1981.
[30] T.F. Ardyukoiva, et al., Atlas of Spectra of Aromatic and Heterocyclic Compounds, Nauka Sib. otd., Novosibirsk, 1973.
[31] Jag Mohan, Organic Spectroscopy—Principles and Applications, second ed., Narosa Publishing House, NewDelhi, 2001.
[32] D.N. Sathyanarayana, vibrational spectroscopy theory and application, New Age International publishers, New Delhi (2004).
[33] S. Ramalingam, S. Periandy, S. Mohan, Spectrochimica Acta Part A 77 (2010) 73–81.
[34] A.R. Prabakaran, S. Mohan, Indian Journal of Physics, 63B (1989) 468-473.
[35] A. Mikhail et al, spectrochemicaActa Part A 77 (2010) 965-972
[36] Manohar et al, spectrochemica Act Part A 71 (2008) 110).
[37] S. Ahmad, S. Mathew, P.K. Verma, Indian Journal of Pure and Applied Physics, 30 (1992) 764-770.
[38] S. Ramalingam, S. Periandy, S. Sugunakala, T. Prabhu, M. Bououdina, Spectrochimica Acta Part A: Molecular and Biomolecular Spectroscopy 115 (2013) 118–135.
[39] Jean, Yvesand and Volatron, François. An Introduction to Molecular Orbitals. Oxford University Press. 11.03. 2005.
[40] E. Scrocco, J. Tomasi, Adv. Quant. Chem. (1979) 11–115.
[41] N. Okulik, A.H. Jubert, Internet Electron. J. Mol. Des. (2005) 4–17.